Study on the System Efficiency of the Capacitive Pulsed-Power Supply

Chen Gong, Xinjie Yu, *Member, IEEE*, and Xiucheng Liu

***Abstract*— Electromagnetic railgun systems based on capacitive pulsed-power supply (CPPS) have obtained widespread applications because of its obvious advantages over the inductive ones on mature technology, operational reliability, and feasible financial condition. However, the existing CPPS-based electromagnetic railgun system works with low efficiency. In this paper, systematical studies on the CPPS in the synchronously triggered electromagnetic railgun system with constant volume and in the time-delay-triggered electromagnetic railgun system with automatic segmentation are proposed, respectively. In the synchronously triggered electromagnetic railgun system, all pulse-forming units (PFUs) are supposed to be triggered synchronously and the load is simplified as a resistor first. Then, the system performance criteria, i.e., the launch velocity of the armature v_{end} and the system efficiency η, are expressed as the function of four independent system variables: 1) the capacitance of each PFU C; 2) the precharged voltage U_C of capacitors; 3) the rail length l; and 4) the armature mass m. The relationship between η (or v_{end}) and any two independent variables can be found under the environment of MATLAB R2012a by fixing the other two parameters. The results are then verified under the environment of Simplorer 8. These figures can be used to instruct the design of the pulsed-power supply for a designated load or the railgun for a designated source. In the time-delay-triggered electromagnetic railgun system, the principle of automatic segmentation is proposed. According to the segmentation principle, the simulation results under the environment of Simplorer 8 are given for comparison. The paper can provide a theoretical foundation for the future designs to get higher system efficiency.**

***Index Terms*— Capacitive pulsed-power supply (CPPS), electromagnetic railgun, synchronously triggered, system efficiency, time delay triggered.**

I. Introduction

COMPARED with inductive pulsed-power supply, capacitive pulsed-power supply (CPPS) has obvious advantages on mature technology, operational reliability, and feasible financial condition [1]–[3], thus obtaining more widespread applications. However, the existing CPPS-based electromagnetic railgun system works with low efficiency. In general, the effective energy, or rather the kinetic energy finally gained by the armature, only accounts for 20% of the total system energy, or even lower [4].

Manuscript received October 11, 2014; revised December 20, 2014; accepted December 25, 2014. Date of publication March 12, 2015; date of current version May 6, 2015. This work was supported in part by the Tsinghua University Initiative Scientific Research Program 20121087927 and in part by the National Natural Science Foundation of China under Project 51377087.

The authors are with the State Key Laboratory of Power, Department of Electrical Engineering, Tsinghua University, Beijing 100084, China (e-mail: vera921023@163.com; yuxj@tsinghua.edu.cn; xcliu@tsinghua.edu.cn).

Color versions of one or more of the figures in this paper are available online at http://ieeexplore.ieee.org.

Digital Object Identifier 10.1109/TPS.2015.2409093

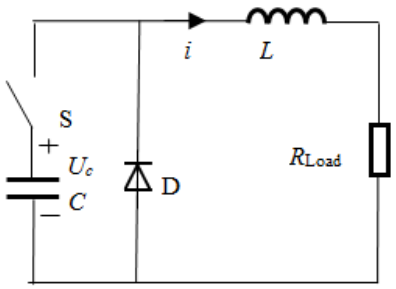

Fig. 1. Topology of the PFU circuit.

With the development of the electromagnetic railgun, the system based on CPPS has required better and better properties, especially a higher efficiency. Until now, there have been two main strategies to improve the system efficiency [5]–[8]: 1) reduce the loss of system energy during the launch and 2) restore the residual energy remaining in the system after the launch [3]. However, so far, almost all of the currently published related studies merely provide one or several experimental schemes to increase the system efficiency. There are a few studies taking consideration of the system efficiency systematically in terms of the circuit topology and analytical expression. It is necessary to do analysis and research on the system efficiency from a theoretical point of view.

In this paper, systematical studies on the CPPS in a 1-MJ synchronously triggered electromagnetic railgun system and in the time-delay-triggered electromagnetic railgun system with automatic segmentation are proposed, respectively.

II. Synchronously Triggered Model

The existing simulation model of CPPS-based electromagnetic railgun system is mainly composed of two primary parts, namely, CPPS with initial energy storage and the railgun load.

The basic module of CPPS is the pulse-forming unit (PFU). In CPPS, multiple PFUs connected in parallel are separated into segments and every PFU in the same segment has the same triggering time. The topology of the PFU is shown in Fig. 1. The energy storage capacitor C consists of a single or a plurality of capacitors connected in series or in parallel, with precharged voltage U_C. The pulse-forming inductor L takes control of the output waveform with its pulsewidth and amplitude, and restricts the spreading of malfunctions. The diode D avoids charging C reversely, thus protecting the capacitor [3], [4] and improving the transmission efficiency. The railgun load can roughly be equivalent to a 1-mΩ resistor R_{Load} [9]–[11].

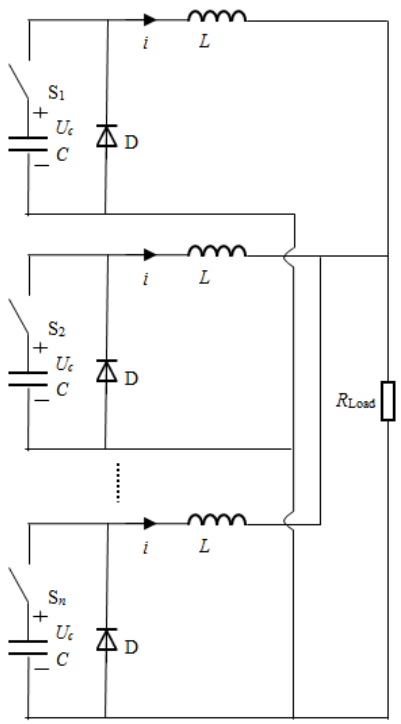

Fig. 2. Synchronously triggered model of CPPS-based electromagnetic railgun system.

All PFUs work through two stages: 1) an Resistor-inductor-capacitor (RLC) second-order circuit with precharged voltage U_C in capacitors C and 2) nearly the same as an RL first-order circuit with remaining energy storage in inductors L. The discharge end of the capacitors is the turning point of the two stages. Therefore, the capacitive energy in C is transferred to the inductive energy in L during the first one quarter period of the second-order circuit, which is the rising time of the current wave. Then the converting inductance value L of each PFU can be determined by the predefined rising time, which is the proper value for most realistic systems, and C.

Assuming that the pulsed-power supply system consists of n PFUs shown in Fig. 2, it can be briefly analyzed by the principles of the synchronously triggered model as follows.

Since all PFUs are the same and they are triggered synchronously and discharging in parallel, according to the circuit symmetry principle, the outflow of PFUs are equal. When n PFUs are discharging in parallel, we can assume that the second-order outflow of each PFU is i_1, and the first-order outflow is i_2. For example, the circuit consisting of the first PFU and its load can be taken as an example. The second-order discharge process of each module is analyzed as follows:

$$\frac{d^2U_C}{dt^2}+\frac{R+nR_{\text{Load}}}{L}\frac{dU_C}{dt}+\frac{1}{LC}U_C=0 \tag{1}$$

where R is the equivalent resistance of inductance L. For there are n PFUs discharging in parallel to a single load with the value of R_{Load}, the equivalent load value for a single PFU is nR_{Load}.

The time variable t in (1) represents the closed time of the discharge switches, which is the start time of second-order discharge and is the armature run time. In the following discussions, $t_{1\text{end}}$ represents the time when capacitor C discharges completely to zero, and is considered as the time when the second-order discharge ends and the first-order discharge starts; $t_{2\text{end}}$ represents the armature launch time.

When n PFUs are triggered synchronously and discharging, the second-order outflow of each PFU can be obtained by the following:

$$i_1=\frac{U_C}{\omega L}e^{-\alpha t}\sin\omega t \quad (0\le t<t_{1\text{end}}) \tag{2}$$

where

$$\alpha=\frac{R+nR_{\text{Load}}}{2L},\quad \omega_0=\frac{1}{\sqrt{LC}}$$
$$\omega=\sqrt{\omega_0^2-\alpha^2},\quad t_{1\text{end}}=\frac{\pi-\arctan\left(\frac{\omega}{\alpha}\right)}{\omega}. \tag{3}$$

Similarly, the first-order outflow of each PFU when n PFUs are triggered synchronously and discharging is described as follows:

$$i_2=\frac{U_C}{\omega L}e^{-\alpha t_{1\text{end}}}\sin(\omega t_{1\text{end}})e^{-\frac{R+nR_{\text{Load}}}{L}(t-t_{1\text{end}})} \quad (t_{1\text{end}}\le t\le t_{2\text{end}}). \tag{4}$$

Then the load current of the railgun system i can be given as

$$i=\begin{cases}n\dfrac{U_C}{\omega L}e^{-\alpha t}\sin\omega t & (0\le t<t_{1\text{end}})\\ n\dfrac{U_C}{\omega L}e^{-\alpha t_{1\text{end}}}\sin(\omega t_{1\text{end}})e^{-\frac{R+nR_{\text{Load}}}{L}(t-t_{1\text{end}})} & (t_{1\text{end}}\le t\le t_{2\text{end}}).\end{cases} \tag{5}$$

III. System Efficiency of the Synchronously Triggered Capacitive Pulsed-Power Supply

Assuming m represents the armature mass, L' represents the rail inductance gradient, according to the principle of dynamics, the force in the armature can be described as in the following equation and the armature acceleration a can also be obtained [12]–[14]:

$$F=\frac{1}{2}L'i^2=ma \tag{6}$$
$$a=\frac{L'i^2}{2\,m}. \tag{7}$$

The system launch process can be divided into two stages: 1) the second-order discharge stage and 2) the first-order discharge stage. The following analysis and solving is according to different periods of the process. By substituting (5) into (7), the acceleration a can be obtained as follows:

$$a=\begin{cases}\dfrac{L'n^2U_C^2}{2m\omega^2L^2}e^{-2\alpha t}\sin^2\omega t & (0\le t<t_{1\text{end}})\\ \dfrac{L'n^2U_C^2e^{-2\alpha\cdot t_{1\text{end}}}\sin^2(\omega t_{1\text{end}})}{2m\omega^2L^2}e^{-\frac{2(R+nR_{\text{Load}})}{L}(t-t_{1\text{end}})} & (t_{1\text{end}}\le t\le t_{2\text{end}}).\end{cases} \tag{8}$$

Speed is the integral of the acceleration of time. Therefore, we can use the time segment integral of

$$v=\begin{cases}\dfrac{L'n^2U_C^2}{2m\omega^2L^2}\displaystyle\int_{x=0}^{x=t}e^{-2\alpha x}\sin^2\omega x dx & (0\le t<t_{1\mathrm{end}})\\ \dfrac{L'n^2U_C^2}{2m\omega^2L^2}\left[\displaystyle\int_{x=0}^{x=t_{1\mathrm{end}}}e^{-2\alpha x}\sin^2\omega x dx+e^{-2\alpha t_{1\mathrm{end}}}\sin^2(\omega t_{1\mathrm{end}})\int_{x=t_{1\mathrm{end}}}^{x=t}e^{-\frac{2(R+nR_{\mathrm{Load}})}{L}(x-t_{1\mathrm{end}})}dx\right] & (t_{1\mathrm{end}}\le t\le t_{2\mathrm{end}})\end{cases}\Rightarrow$$

$$v=\begin{cases}\dfrac{-L'n^2U_C^2e^{-2\alpha t}}{8\ mL^2\omega_0^2}\left[\dfrac{\alpha(1-\cos(2\omega t))}{\omega^2}-\dfrac{1}{\alpha e^{-2\alpha t}}+\dfrac{1}{\alpha}+\dfrac{\sin(2\omega t)}{\omega}\right] & (0\le t<t_{1\mathrm{end}})\\ \dfrac{-L'n^2U_C^2e^{-2\alpha t_{1\mathrm{end}}}}{8\ mL^2\omega_0^2}\left[\dfrac{\alpha(1-\cos(2\omega t_{1\mathrm{end}}))}{\omega^2}-\dfrac{1}{\alpha e^{-2\alpha t_{1\mathrm{end}}}}+\dfrac{1}{\alpha}+\dfrac{\sin(2\omega t_{1\mathrm{end}})}{\omega}\right]\\ \quad+\dfrac{L'n^2U_C^2\sin^2(\omega t_{1\mathrm{end}})e^{-2\alpha t_{1\mathrm{end}}}}{4\ mL\omega^2(R+nR_{\mathrm{Load}})}\left(1-e^{-\frac{2(R+nR_{\mathrm{Load}})}{L}(t-t_{1\mathrm{end}})}\right) & (t_{1\mathrm{end}}\le t\le t_{2\mathrm{end}})\end{cases}\tag{9}$$

$$v_{\mathrm{end}}=\frac{-L'n^2U_C^2e^{-2\alpha t_{1\mathrm{end}}}}{8\ mL^2\omega_0^2}\left[\frac{\alpha(1-\cos(2\omega t_{1\mathrm{end}}))}{\omega^2}-\frac{1}{\alpha e^{-2\alpha t_{1\mathrm{end}}}}+\frac{1}{\alpha}+\frac{\sin(2\omega t_{1\mathrm{end}})}{\omega}\right]+\frac{L'n^2U_C^2\sin^2(\omega t_{1\mathrm{end}})e^{-2\alpha t_{1\mathrm{end}}}}{4\ mL\omega^2(R+nR_{\mathrm{Load}})}\left(1-e^{-\frac{2(R+nR_{\mathrm{Load}})}{L}(t_{2\mathrm{end}}-t_{1\mathrm{end}})}\right)\tag{10}$$

$$S=\begin{cases}\dfrac{-L'n^2U_C^2}{8\ mL^2\omega_0^2}\displaystyle\int_{x=0}^{x=t}\left(\frac{\alpha(1-\cos(2\omega x))e^{-2\alpha x}}{\omega^2}-\frac{1}{\alpha}+\frac{e^{-2\alpha x}}{\alpha}+\frac{\sin(2\omega x)e^{-2\alpha x}}{\omega}\right)dx & (0\le t<t_{1\mathrm{end}})\\ \dfrac{-L'n^2U_C^2}{8\ mL^2\omega_0^2}\displaystyle\int_{x=0}^{x=t_{1\mathrm{end}}}\left(\frac{\alpha(1-\cos(2\omega x))e^{-2\alpha x}}{\omega^2}-\frac{1}{\alpha}+\frac{e^{-2\alpha x}}{\alpha}+\frac{\sin(2\omega x)e^{-2\alpha x}}{\omega}\right)dx\\ \quad+\dfrac{L'n^2U_C^2e^{-2\alpha t_{1\mathrm{end}}}}{8\ mL^2\omega_0^2\omega^2}\displaystyle\int_{x=t_{1\mathrm{end}}}^{x=t}\left[\frac{\omega^2}{\alpha e^{-2\alpha t_{1\mathrm{end}}}}+\frac{2\omega_0^2L\sin^2(\omega t_{1\mathrm{end}})}{(R+nR_{\mathrm{Load}})}\left(1-e^{-\frac{2(R+nR_{\mathrm{Load}})}{L}(t-t_{1\mathrm{end}})}\right)\right.\\ \qquad\left.-\omega\sin(2\omega t_{1\mathrm{end}})-\dfrac{\omega^2}{\alpha}-\alpha(1-\cos(2\omega t_{1\mathrm{end}}))\right]dx & (t_{1\mathrm{end}}\le t\le t_{2\mathrm{end}})\end{cases}\Rightarrow$$

$$S=\begin{cases}\dfrac{L'n^2U_C^2e^{-2\alpha t_{1\mathrm{end}}}}{16\ mL^2\omega_0^4}\left[\dfrac{\alpha^2(1-\cos(2\omega t_{1\mathrm{end}}))}{\omega^2}+2+\dfrac{2t_{1\mathrm{end}}\omega^2}{\alpha e^{-2\alpha t_{1\mathrm{end}}}}+\dfrac{\omega^2(e^{-2\alpha t_{1\mathrm{end}}}-1)}{\alpha^2e^{-2\alpha t_{1\mathrm{end}}}}+\cos(2\omega t_{1\mathrm{end}})\right.\\ \qquad\left.+\dfrac{2\alpha t_{1\mathrm{end}}-3}{e^{-2\alpha t_{1\mathrm{end}}}}+\dfrac{2\alpha\sin(2\omega t_{1\mathrm{end}})}{\omega}\right] & (0\le t<t_{1\mathrm{end}})\\ \dfrac{L'n^2U_C^2e^{-2\alpha t_{1\mathrm{end}}}}{16\ mL^2\omega_0^4}\left[\dfrac{\alpha^2(1-\cos(2\omega t_{1\mathrm{end}}))}{\omega^2}+2+\dfrac{2t_{1\mathrm{end}}\omega^2}{\alpha e^{-2\alpha t_{1\mathrm{end}}}}+\dfrac{\omega^2(e^{-2\alpha t_{1\mathrm{end}}}-1)}{\alpha^2e^{-2\alpha t_{1\mathrm{end}}}}+\cos(2\omega t_{1\mathrm{end}})\right.\\ \qquad\left.+\dfrac{2\alpha t_{1\mathrm{end}}-3}{e^{-2\alpha t_{1\mathrm{end}}}}+\dfrac{2\alpha\sin(2\omega t_{1\mathrm{end}})}{\omega}\right]\\ \quad+\dfrac{L'n^2CU_C^2e^{-2\alpha t_{1\mathrm{end}}}}{4m(R+nR_{\mathrm{Load}})}\left[\dfrac{L\left(e^{-\frac{2(R+nR_{\mathrm{Load}})}{L}(t-t_{1\mathrm{end}})}-1\right)}{2(R+nR_{\mathrm{Load}})}+t-t_{1\mathrm{end}}\right]\\ +\dfrac{L'n^2CU_C^2e^{-2\alpha t_{1\mathrm{end}}}}{8\ mL\omega^2\alpha}\left[\alpha^2\cos(2\omega t_{1\mathrm{end}})-\alpha\omega\sin(2\omega t_{1\mathrm{end}})+\dfrac{\omega^2}{e^{-2\alpha t_{1\mathrm{end}}}}-\alpha^2-\omega^2\right](t-t_{1\mathrm{end}}) & (t_{1\mathrm{end}}\le t\le t_{2\mathrm{end}})\end{cases}\tag{11}$$

the acceleration a to obtain the armature velocity v, as in (9), shown at the top of the page. Assuming the armature launch time is $t_{2\mathrm{end}}$, with (9), the armature launch velocity v can be obtained as (10), shown at the top of the page.

Then we can use the time segment integral of the velocity v to acquire the armature's moving distance S, as in (11), shown at the top of the page. After we put launch time $t_{2\mathrm{end}}$ into (11) and consider that the corresponding distance of the armature is the rail length l, (12), shown at the top of the next page, can be acquired. The system efficiency of the synchronously triggered CPPS in the electromagnetic railgun system can be described as (13), shown at the top of the next page.

We can see from (10), (12), and (13) that since the rising edge slope of the pulse discharge current waveform is a constant value, namely, LC = constant, the influential factors of system efficiency η are four independent parameters: 1) the capacitance of each PFU C; 2) the precharged voltage U_C of capacitors; 3) the rail length l; and 4) the armature mass m.

We can choose any two of the influential factors as independent variables, such as m and U_C, and set both l and C to be constants. Other system parameters can be expressed as the function of m and U_C. According to (12), by numerical calculation, we can obtain $t_{2\mathrm{end}}$ corresponding to m and U_C with arbitrary values. After acquiring launch time $t_{2\mathrm{end}}$, we can obtain v_{end} corresponding to m and U_C with arbitrary values according to (10). Then the relationship of velocity v_{end}, mass m, and voltage U_C can be given as $m-U_C-v_{\mathrm{end}}$.

$$l = \frac{L'n^2U_C^2e^{-2\alpha t_{1\text{end}}}}{16\ mL^2\omega_0^4}\left[\frac{\alpha^2(1-\cos(2\omega t_{1\text{end}}))}{\omega^2} + 2 + \frac{2t_{1\text{end}}\omega^2}{\alpha e^{-2\alpha t_{1\text{end}}}} + \frac{\omega^2(e^{-2\alpha t_{1\text{end}}}-1)}{\alpha^2 e^{-2\alpha t_{1\text{end}}}} + \cos(2\omega t_{1\text{end}}) + \frac{2\alpha t_{1\text{end}}-3}{e^{-2\alpha t_{1\text{end}}}} + \frac{2\alpha\sin(2\omega t_{1\text{end}})}{\omega}\right] + \frac{L'n^2CU_C^2e^{-2\alpha t_{1\text{end}}}}{4m(R+nR_{\text{Load}})}\left[\frac{L\left(e^{-\frac{2(R+nR_{\text{Load}})}{L}(t_{2\text{end}}-t_{1\text{end}})}-1\right)}{2(R+nR_{\text{Load}})} + t_{2\text{end}} - t_{1\text{end}}\right] + \frac{L'n^2CU_C^2e^{-2\alpha t_{1\text{end}}}}{8\ mL\omega^2\alpha}\left[\alpha^2\cos(2\omega t_{1\text{end}}) - \alpha\omega\sin(2\omega t_{1\text{end}}) + \frac{\omega^2}{e^{-2\alpha t_{1\text{end}}}} - \alpha^2 - \omega^2\right](t_{2\text{end}} - t_{1\text{end}}) \tag{12}$$

$$\eta = \frac{W_k}{W_s} = \frac{U_C^2L'^2n^4e^{-4\alpha t_{1\text{end}}}}{16\ mL^4C\omega_0^4}\left[\frac{\omega_0^2L\sin^2(\omega t_{1\text{end}})}{\omega^2(R+nR_{\text{Load}})}\left(1-e^{-\frac{2(R+nR_{\text{Load}})}{L}(t_{2\text{end}}-t_{1\text{end}})}\right) + \frac{(1-e^{-2\alpha t_{1\text{end}}})}{2\alpha e^{-2\alpha t_{1end}}} - \frac{\alpha(1-\cos(2\omega t_{1\text{end}}))}{2\omega^2} - \frac{\sin(2\omega t_{1\text{end}})}{2\omega}\right]^2 \tag{13}$$

Similarly, since launch time $t_{2\text{end}}$ has been calculated, we can obtain η corresponding to the m and U_C with arbitrary value, according to (13). Then the relationship of efficiency η, mass m, and voltage U_C can be given as $m - U_C - \eta$.

Using the method above, we can calculate the launch velocity of the armature v_{end} and the system efficiency η, corresponding to the m and U_C with arbitrary values. After selecting any two of the influential factors as independent variables, we can set the other two influential factors as constants and other system parameters can be expressed as the function of the two independent variables, and the method above is also suitable.

IV. Relationship Between the Efficiency and Influential Factors for 1-MJ System With Simulation Verification

A 1-MJ synchronously triggered system is taken for an example to study the influential relationship of the armature mass m, the precharged voltage U_C of capacitors, and the system efficiency η, according to the above theoretical analysis. The system parameter setting is shown in Table I.

Carrying out theoretical numerical computation on the platform of MATLAB R2012a, the relationship of mass m, voltage U_C, and velocity v_{end} of the 1-MJ system is shown in Fig. 3.

Similarly, the relationship of mass m, voltage U_C, and efficiency η of the 1-MJ system can be obtained and is shown in Fig. 4.

According to the result of MATLAB R2010a, we can select points to carry out simulation on the platform of Simplorer 8 to verify the correctness of previous deduction.

Here, we take four points in Fig. 4 for verification. For each point, with the coordinates in Fig. 4 and the parameters in Table I, we can do the simulation in Simplorer and compare the results with those obtained in MATLAB. The comparisons are shown in Table II. It is easy to see that the error ratio between the theoretical equations and the simulation results is acceptable, thus proving that the theoretical equations are correct and effective.

It needs to be noted that to get clearer representation, the discussion here does not consider the current limit on the rail. That is to say, all the PFUs are discharged at the same time. In the real situation, this may cause the erosion and gouging in the rails and is unrealistic. However, this discussion is still useful because it points out the upper bound for the system efficiency.

V. Time-Delay-Triggered Model

Establishing the time-delay-triggered model is to segment PFUs and arrange the trigger timing automatically for the electromagnetic railgun system, making sure that the load current is within the reasonable scope, for example, in the interval (550 and 750 kA), and it is feasible enough to launch the armature. Generally speaking, the square wave is considered to be the ideal waveform of load current, and thus, the principle of the automatic segmentation in the time-delay-triggered model is to converge to the ideal square wave.

Assuming that the pulsed-power supply system consists of n PFUs and can be divided into k segments discharging time delay shown in Fig. 5, it can be briefly analyzed by the principles of the time-delay-triggered model as follows.

The time-delay-triggered model parameter setting is shown in Table III.

Define $\Delta t_{d1} = 0$ and $t_{\text{end}0} = 0$, we can obtain the following:

$$\begin{aligned} t_{dk} &= t_{\text{end}k-1} + \Delta t_{dk} \\ t_{\text{end}k} &= t_{dk} + \Delta t_{\text{end}k} \quad (k \geq 1). \end{aligned} \tag{14}$$

Then, the second-order outflow of segment k can be obtained as follows:

$$i_{k1} = \frac{n_k u}{\omega_k L}e^{-\alpha_k(t-t_{dk})}\sin(\omega_k(t-t_{dk})) \tag{15}$$

where

$$\begin{aligned} \alpha_k &= \frac{R+n_kR_{\text{load}}}{2L}, \quad \omega_0 = \sqrt{\frac{1}{LC}} \\ \omega_k &= \sqrt{\omega_0^2-\alpha_k^2}, \quad \Delta t_{\text{end}k} = \frac{\pi - \arctan\left(\frac{\omega_k}{\alpha_k}\right)}{\omega_k}. \end{aligned} \tag{16}$$

TABLE I
SYSTEM PARAMETER SETTING

Parameter	Value	Unit
system capacity (W_s)	1	MJ
PFU capacitance (C)	2	mF
PFU inductance (L)	50	μH
PFU resistance (R)	3	mΩ
load resistance (R_{Load})	1	mΩ
rail length (l)	4	m
PFU number (n)	$n = \left\lfloor \frac{2W_s}{CU_C^2} \right\rfloor$	

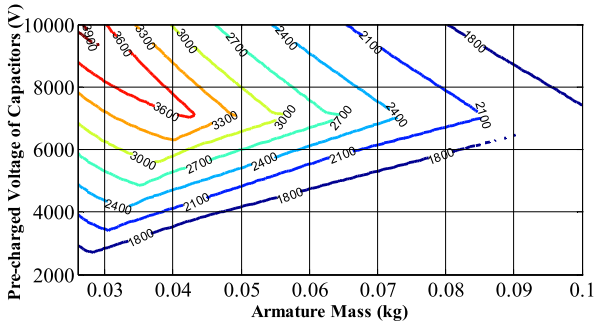

Fig. 3. Relationship $m - U_C - v_{end}$ of the 1-MJ system ($l = 4$ m, $C = 2$ mF).

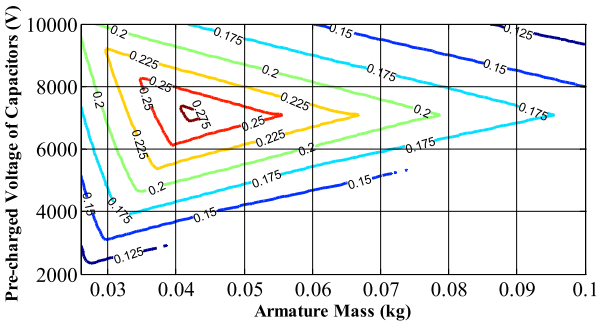

Fig. 4. Relationship $m - U_C - \eta$ of the 1-MJ system ($l = 4$ m and $C = 2$ mF).

TABLE II
DATA COMPARISON BETWEEN MATLAB R2010a AND SIMPLORER 8

Matlab (v_{end}, η) Unit (m/s, %)	Simplorer®8 (v_{end}, η) Unit (m/s, %)	Error Ratio (δ_v, δ_η) $\delta = \frac{M-S}{M}$
(3597.5, 28.05)	(3633.2, 28.36)	(-0.99, -1.11) %
(3798.3, 24.42)	(3791.8, 24.47)	(0.17, -0.20)%
(3812.9, 21.63)	(3726.1, 21.10)	(2.28, 2.45)%
(2268.2, 20.07)	(2274.4, 20.15)	(-0.27, -0.40)%

Similarly, the first-order outflow and the peak current of segment k can be obtained, respectively, by the following:

$$i_{k2} = \frac{n_k u}{\omega_k L} e^{-\alpha_k \Delta t_{endk}} \sin(\omega_k \Delta t_{endk}) e^{-\frac{R+n_k R_{load}}{L}(t-t_{endk})} \quad (17)$$

$$i_{max\,k} = \frac{n_k u}{\omega_k L} e^{-\alpha_k \Delta t_{max\,k}} \sin(\omega_k \Delta t_{max\,k}). \quad (18)$$

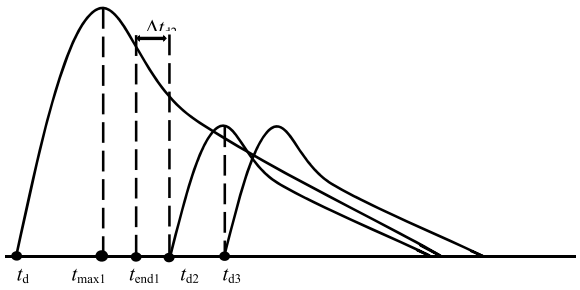

Fig. 5. Discharging current of time-delay-triggered model.

TABLE III
TIME-DELAY-TRIGGERED MODEL PARAMETER SETTING

Parameter	Description
k	Segment number
t_{dk}	Trigger time of segment k
t_{endk}	Time point of segment k at which the second-order discharge ends
$t_{max\,k}$	Time point of segment k at which the segment current reaches the peak
Δt_{dk}	Time from t_{endk-1} to t_{dk}
Δt_{endk}	Time from t_{dk} to t_{endk}
$\Delta t_{max\,k}$	Time from t_{dk} to $t_{max\,k}$

There is a basic consensus on the system that the first segment can be thought of as the main section of the whole pulsed-power supply system. It determines the load current energy level, or even the peak of the load current, mainly because it contains large number of PFUs. In addition, each segment after the first one can be thought as an auxiliary section of the pulsed-power supply system, whose main role is to compensate for the falling current of the previous segment, because the PFU number in these auxiliary sections are relatively small.

Because of the particularity of the first segment, we take the time point as the trigger time of the second segment, when the load current, namely, the current of first segment, falls down to the lowest value of feasible load current I_{limit}. After the second segment, we take the time point as the trigger time of segment k, when segment $k-1$ reaches the peak current, where k is the segment number and $k \geq 3$. The reasons are as follows. When segment k reaches the current peak, segments from 1 to $k-1$ must have been in the declining first-order stage, and thus the load current that is formed by current of all segments must be in the reducing state. It is the time to trig segment k to make compensation. As it is easy to see that the trigger time of segment 1 $t_{d1} = 0$ and there is no big difference between t_{endk} and $t_{max\,k}$, we can simplify the trigger time as follows:

$$t_{dk} = t_{endk-1} = t_{max\,k-1} \quad (k \geq 3). \quad (19)$$

Then we discuss the PFU number of each segment. According to (18), it is not difficult to obtain the PFU number of segment $1 n_1$ by solving the equation $i_{max\,1} = I_{peak}$,

TABLE IV
STANDARD SYSTEM PARAMETER SETTING

Parameter	Value	Unit
system capacity (W_s)	0.75	MJ
PFU capacitance (C)	2	mF
PFU inductance (L)	50	μH
PFU resistance (R)	20	mΩ
load resistance (R_{Load})	1	mΩ
capacitor pre-charged voltage (U_C)	5	kV

TABLE V
STANDARD SYSTEM TRIGGER TIMING SETTING

Segment	PFU number	Trigger Time
1	20	0 ms
2	3	0.50 ms
3	2	0.60 ms
4	2	0.70 ms
5	2	0.85 ms
6	1	0.90 ms

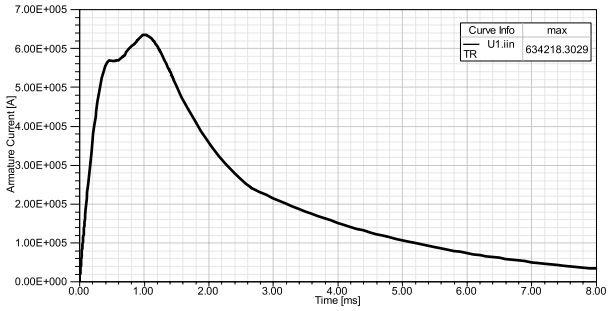

Fig. 6. Load current of the standard system.

where I_{peak} is the highest value of feasible load current. It can be understood like this, the current increment that segment 1 need to provide is $\Delta i_1 = I_{\text{peak}} - 0$ and the peak current that segment 1 can provide is $i_{\max 1}$, so we match them as the equation $i_{\max 1} = \Delta i_1 = I_{\text{peak}}$ to find out how many PFUs can provide the current value, that is n_1.

Assume the PFU number of segment k as n_k, where $k \geq 2$. The current increment that segment k need to compensate is $\Delta i_k = I_{\text{peak}} - I_{\text{limit}}$. Therefore, we can solve the similar equation as $i_{\max k} = \Delta i_k = I_{\text{peak}} - I_{\text{limit}}$ to figure out n_k. If the PFU resistance R is bigger enough than the load resistance R_{Load}, according to the equation $\alpha_k = (R + n_k R_{\text{load}}/2L)$, we can use the proportional equation $(n_1/n_k) = (\Delta i_1/\Delta i_k)$ to calculate n_k approximately. Thus, the PFU number of segment k n_k can be described as follows:

$$n_k = \frac{\Delta i_k}{\Delta i_1} n_1 = \frac{I_{\text{peak}} - I_{\text{limit}}}{I_{\text{peak}}} n_1 \quad (k \geq 2). \tag{20}$$

VI. SIMULATION VERIFICATION AND ANALYSIS OF THE TIME-DELAY-TRIGGERED MODEL

For comparison convenience, we make an existing 0.75-MJ CPPS system as the standard system. The parameter setting of the standard system provided by relevant units is shown in Table IV.

The trigger timing setting of the standard system is shown in Table V.

The load current of the standard system is shown in Fig. 6.

By the method given in this paper, we can calculate automatically and obtain a new set of trigger timing for the 750-kJ system, as shown in Table VI. And the load current of the new trigger-timing-setting system is shown in Fig. 7.

Similarly, we do the same automatic segmentation for a 1.5-kJ and 3.0-MJ system with the same parameter setting as the standard system. Figs. 8 and 9 show the load current of these two systems, respectively.

TABLE VI
NEW SET OF TRIGGER TIMING

Segment	PFU number	Trigger Time
1	23	0 ms
2	4	0.61 ms
3	3	1.21 ms

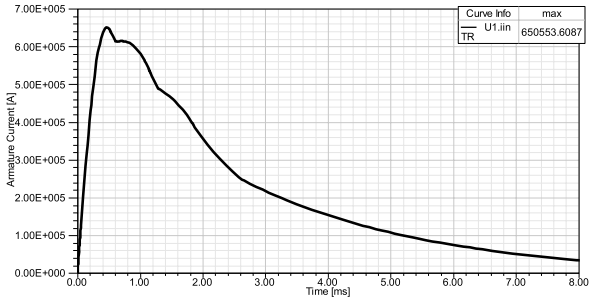

Fig. 7. Load current of the new trigger-timing-setting system.

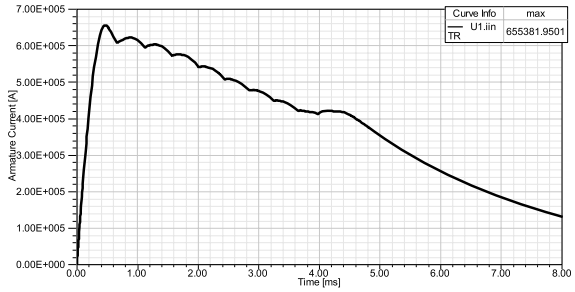

Fig. 8. Load current of the 1.5-MJ system.

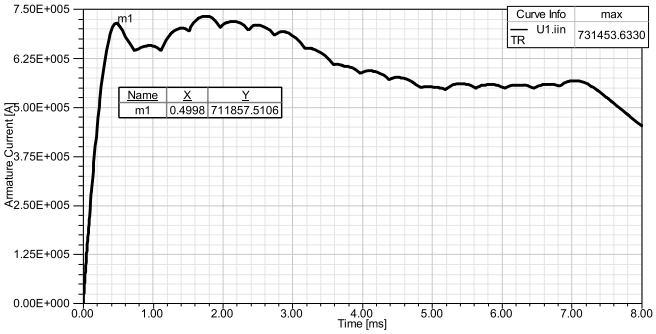

Fig. 9. Load current of the 3.0-MJ system.

From the above simulation waveforms, we can easily see that the principle proposed in this paper can meet the current limiting conditions, the realization of automatic segmentation and the time-delay-triggered design in the electromagnetic railgun system with the CPPS. The load current based on the segmentation principle is feasible enough to launch the armature.

VII. Conclusion

In this paper, study on the CPPS in the electromagnetic railgun system is discussed in detail.

On the premise that the system capacity is 1 MJ and the rising edge slope of the pulse discharge current waveform is a constant value, namely, $LC =$ constant, we make the formula derivation of the system efficiency of the synchronously triggered CPPS in the electromagnetic railgun system and obtain the theoretical equations.

We draw the relationship figures between the system performance criteria and influential factors for 1-MJ system based on MATLAB R2010a and make simulation verification based on Simplorer 8. The relationship of the armature mass m, the precharged voltage U_C of capacitors, and the armature velocity v_{end} for 1-MJ system, or rather $m - U_C - v_{\text{end}}$, and the relationship of the armature mass m, the precharged voltage U_C of capacitors, and the system efficiency η for 1 MJ system, or rather $m - U_C - \eta$, are obtained in the paper. With Figs. 3 and 4, for the design and operation of a certain system, we can easily obtain the independent variables corresponding to the maximum velocity or the maximum efficiency, which has important theoretical and practical meaning for system design and operation.

This paper opens a door to study synchronously triggered systems. We can obtain the relationship between η (or v_{end}) and any two of the influential factors through the theoretical equations. With or without constant capacity, these equations can provide existing systems with more efficient solutions, and also be used in parameter optimization designs for new systems, including the source side and the load side.

As for time-delay-triggered system, a kind of feasible principle to divide PFUs into segments automatically is proposed in this paper, considering the ideal square wave as the target waveform. The simulation results show that the principle works well and the load wave obtained by the principle can meet the launch conditions.

Although some principles to segment PFUs automatically is proposed in this paper, the theoretical equations are not given yet. The theoretical analysis on models triggered with delay pulse will be taken into consideration in the future.

References

[1] R. A. Marshall and W. Ying, *Railguns: Their Science and Technology*. Beijing, China: Machine Press, 2003.

[2] W. A. Walls, W. F. Weldon, S. B. Pratap, M. Palmer, and D. Adams, "Application of electromagnetic guns to future naval platforms," *IEEE Trans. Magn.*, vol. 35, no. 1, pp. 262–267, Jan. 1999.

[3] H. D. Fair, "Electromagnetic launch science and technology in the United States enters a new era," *IEEE Trans. Magn.*, vol. 41, no. 1, pp. 158–164, Jan. 2005.

[4] G. Chen, Y. Xinjie, and L. Xiucheng, "Continuous emission scheme and its simulation for capacitor-based railgun system," in *Proc. 7th Conf. Theory Adv. Technol. Elect. Eng.*, 2013.

[5] M. Crawford *et al.*, "The design and testing of a large-caliber railgun," *IEEE Trans. Magn.*, vol. 45, no. 1, pp. 256–260, Jan. 2009.

[6] T. G. Engel, J. M. Neri, and M. J. Veracka, "The maximum theoretical efficiency of constant inductance gradient electromagnetic launchers," *IEEE Trans. Plasma Sci.*, vol. 37, no. 4, pp. 608–614, Apr. 2009.

[7] P. Liu, J. Li, Y. Gui, S. Li, Q. Zhang, and N. Su, "Analysis of energy conversion efficiency of a capacitor-based pulsed-power system for railgun experiments," *IEEE Trans. Plasma Sci.*, vol. 39, no. 1, pp. 300–303, Jan. 2011.

[8] T. G. Engel, J. M. Neri, and M. J. Veracka, "The velocity and efficiency limiting effects of magnetic diffusion in railgun sliding contacts," in *Proc. 14th Symp. Electromagn. Launch Technol.*, Jun. 2008, pp. 1–5.

[9] J. McFarland and I. R. McNab, "A long-range naval railgun," *IEEE Trans. Magn.*, vol. 39, no. 1, pp. 289–294, Jan. 2003.

[10] H. D. Fair, "Electric launch science and technology in the United States," *IEEE Trans. Magn.*, vol. 39, no. 1, pp. 11–17, Jan. 2003.

[11] E. Spahn, M. Lichtenberger, and F. Hatterer, "Pulse forming network for the 10 MJ-railgun PEGASUS," in *Proc. 5th Eur. Symp. Electromagn. Launch Technol.*, 1995, pp. 79–82.

[12] I. R. McNab, S. Fish, and F. Stefani, "Parameters for an electromagnetic naval railgun," *IEEE Trans. Magn.*, vol. 37, no. 1, pp. 223–228, Jan. 2001.

[13] L. D. Thornhill, J. H. Batteh, and D. M. Littrell, "Scaling study for the performance of railgun armatures," *IEEE Trans. Plasma Sci.*, vol. 17, no. 3, pp. 409–421, Jun. 1989.

[14] F. Deadrick, R. Hawke, and J. Scudder, "MAGRAC—A railgun simulation program," *IEEE Trans. Magn.*, vol. 18, no. 1, pp. 94–104, Jan. 1982.

Chen Gong received the B.S. degree in electrical engineering and automation, and the M.S. degree in electrical engineering from Tsinghua University, Beijing, China, in 2012 and 2014, respectively.

Her current research interests include pulsed-power supply.

Xinjie Yu (M'01) received the B.S. and Ph.D. degrees in electrical engineering from Tsinghua University, Beijing, China, in 1996 and 2001, respectively.

He is currently an Associate Professor of Electrical Engineering with Tsinghua University. His current research interests include pulsed-power supply, power electronics, and computational intelligence.

Xiucheng Liu received the B.S., M.S., and Ph.D. degrees in electrical engineering from Tsinghua University, Beijing, China, in 1983, 1989, and 2009, respectively.

He has been an Associate Professor with the Department of Electrical Engineering and Applied Electronics, Tsinghua University, since 1998. His current research interests include pulsed-power supply, and circuit theory and its applications.